

Thermal Imaging of Liquid Steel and Slag in a Pouring Stream

By G. Raymond Peacock
Senior Staff Engineer, Process Analysis Group
LTV Steel Technology Center
LTV Steel Company Inc.
Independence, Ohio

ABSTRACT

Detecting the presence of liquid slag in the pouring or tapping stream of a basic oxygen furnace after steel-making offers a chance to aid the process by maximizing the amount of steel removed from the vessel while minimizing the amount of slag deposited into the holding vessel or ladle. Thermal imaging has been shown capable of real-time images that easily discriminate between the two materials by exploiting their differences in apparent temperature. However, the underlying radiation thermometry theory has yet to be published. Combine this lack of theory with the need for very robust equipment to provide 24/7 uptime and serious obstacles to equipment investment appear. This presentation reviews some basic radiation thermometry theory, along with material properties to show that significant discrimination differences between slag and steel exist in different wavelength passbands. Combining these differences with the imaging, lifetime and cost properties of commercially available devices enables one to develop the necessary tradeoffs between discrimination ability, image quality, equipment reliability and system costs.

Keywords: thermal imaging, near infrared thermal imaging, short wavelength infrared passband, long wavelength infrared passband, spectral radiance, spectral radiance temperature, spectral emissivity, steel, slag

I. INTRODUCTION

The detection of slag in the tap or pouring stream from a steelmaking vessel is an application whose time has arrived. The equipment capability and the need are coincident. Several equipment vendors are supplying or promising equipment.

The main purpose of this paper is to provide sufficient theory to not only understand why and how the application works but to understand the capabilities of proposed thermal imaging equipment solutions. Finally, it appears that an optimum technology solution exists. It is one that is similar to a system described in 1995 at Thermosense XVII, a "Near" infrared wavelength passband imaging system.

II. USE OF THERMAL IMAGING TO DETECT SLAG

Steelmaking in modern, integrated steel plants is performed in large refractory-lined vessels known as Basic Oxygen Furnaces or simply, BOFs. During the processing, a layer of heterogeneous liquid, non-metallic material called slag is developed. Being less dense than the liquid steel, the slag layer floats on the steel.

Steel is removed from the vessel by tipping it and pouring the steel out a side opening, the tap hole, in the furnace wall near the top into a transfer vessel or ladle. Some slag inevitably enters the ladle. The increasing business pressure to be more productive while maintaining high quality in steel products results in the need to minimize the amount of slag poured while maximizing the amount of steel extracted from the BOF.

An operator manually controls the entire pouring, or tapping, practice and judgments about slag entrained into the tap stream are based on visual observation of the tap stream. The steel stream is very bright because its temperature is about 1650°C (~3000°F). It is nearly impossible for an observer to directly see any details, let alone brightness variations, of the stream. Even using a furnace glass filter, the scene visual contrast is quite small and it requires considerable training for an observer to distinguish slag from steel by their brightness differences; slag being brighter than steel because it has a higher emissivity. Routine observations also have been subject to the person-to-person variations and similar problems associated with any observer-based judgment, e.g., concentration and awareness level, reaction time, etc.

About 20 years ago it was shown that an infrared thermal imaging system¹ could perform this measurement readily and provide a far higher contrast image from which an observer could make an easier decision, or upon which an automatic control of the operation could be established. Figure 1 is a copy of the Patent Figure from the 1980 US patent, assigned to Sumitomo Metals Company, which depicts the measurement situation. However, the thermal imaging equipment 20 years ago had neither the reliability nor the ruggedness for regular use in a BOF shop that operates around the clock, 24 hours a day, 7 days per week, as most do.

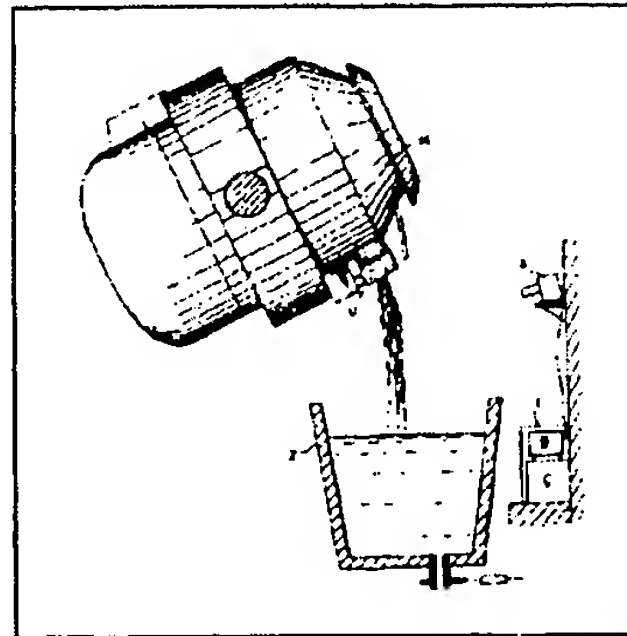


Figure 1. BOF Vessel pouring steel into ladle with IR Camera (A) viewing steel stream

In addition to availability, any equipment used in this application has to cope with long sighting distances, a nearly constant shower of fine dust particles, periodic events with smoke and dust in the sight path, very long signal cable runs and seasonal variations in ambient temperature that can range from -20°C to $+40^{\circ}\text{C}$ in North America (BOF shops are structures essentially open to the environment on several sides and unheated). Finally, ideal equipment should operate with minimal maintenance support and also survive regular high radiant thermal loading from the pouring stream.

The imaging equipment situation has changed radically in the last few years with the development of focal plane array (FPA) cameras with better Mean Time Between Failures (MTBF) and more reliable imaging systems based on them. Steel production needs have become even more pressing than earlier. The result is that several companies are now offering measurement systems that integrate thermal imaging with video archiving of liquid steel pours and provide regular reports of the amount of slag entrained into the ladle. With these new features, this appears to be a growth area for thermal imaging camera suppliers.

A very recent patent², assigned to Bethlehem Steel Company, on the use of IR imaging systems to detect slag in this application, claimed the "Long" ($8\text{-}14\ \mu\text{m}$) wavelength passband, not specifically claimed in the 1980 Sumitomo patent. Bethlehem's new patent also claims rights to any IR imager viewing steel that has an emissivity of less than 0.25. These claims could add licensing costs to any equipment cost in implementing a hardware solution in both the "Long" and "Short" thermal imaging passbands, as will be seen below.

Surprisingly, despite two patents and at least one technical presentation, no complete explanation of how this technique works has been presented beyond the assertion that slag is brighter than steel because of its higher emissivity. Rather, it is like many applications that have been developed by thermal imaging pioneers, it is based on empirical trials. The theory is explained after the interest is created and then measurement optimums are sought.

Now, a new challenge has arisen: which imaging system offers the best choice for a user's needs, especially the tradeoffs between measurement capability, functionality and life cycle costs? Thermal imaging systems, while often easily cost justified, represent significant capital purchases on the part of steel companies and some mechanism for evaluating the performance per unit cost is required. Steel companies are capital-intensive organizations and the expenditure of any capital amount is done carefully with high rate of return projects getting preference.

III. EQUIPMENT OPTIONS

The Imaging Wavelengths and Equipment

Commercial thermal imaging equipment is usually described as “Short” or “Long” wavelength passband equipment. The wavebands referenced are typically 3-5 microns and 8-12 or 8-14 microns, respectively. At the very high temperatures of this application, 1650°C (~3000°F), “Near” IR, 0.7 to 1.0 micron wavelength passband equipment is also a viable candidate since there is a large amount of radiant energy present in the visible and near IR wavelength regions.

Short Wavelength Passband Devices

The 3-5 μm thermal imaging or short wavelength passband has been widely used in many commercial IR cameras and measuring systems for more than 25 years. Typical detector elements have been Indium Antimonide, Lead Selenide and other special photovoltaic sensors. The early devices required cooling to liquid Nitrogen temperature (77 K) to attain the desired responsivities, usually to measure near and sub-ambient temperatures. The early “scanners” were literally that, optical scanning devices using crossed scanning systems and complex electronics to create a 2-D thermal image using a single detector.

Linear detectors arrays have helped reduce the complexity of the scanning devices used to create a 2-D image, but it was not until quite recently that complete 2-dimension (2-D) detector arrays called Focal Plane Arrays (FPA), requiring little to no cooling have become available. Typical detector arrays in Platinum Silicide (Pt/Si) have configurations of 256 x 256 elements. These are remarkable devices and have ushered in a whole new range of applications, especially those needing more reliable equipment. With fewer moving parts and reduced cooling requirements, the new FPA camera markets have expanded and equipment costs have been reduced.

Long Wavelength Passband Devices

The long 8-12 μm and 8-14 μm passband thermal imagers use Mercury-Cadmium-Telluride (MCT or HgCdTe) point detectors and detector arrays and they also required cooling until quite recently. Now, 2-D FPAs such as microbolometers have revolutionized this equipment with 320 x 240 arrays and larger ones promised in the future. Some cooling is still required for best measurement capability, but it is now done with greater reliability and using smaller and more reliable components.

IR Optics & MTBF

Due to the wavelength of the passbands used, the optics for the short and long wavelength systems must be fabricated from infrared transmitting optical materials such as Silicon and Germanium. Such optics are custom made and great care must be taken in their fabrication to assure good imaging properties since they are relatively high index of refraction materials. The basic materials are expensive and when the precision optical fabrication costs are added, most IR optics become very expensive especially when compared to glass optics having similar imaging capabilities. For instance, an 85 mm focal length, f/ 2.0 telephoto lens for a $\frac{1}{2}$ CCD video camera is priced in the \$1000 range, while a comparable IR lens is about 20 times the price.

The early point sensor or linear array sensors with optomechanical scanners were notorious for their relatively short MTBFs. Some vendors expressed times in the range of 2500 hours. The new, FPA cameras promise much longer-lived and more robust equipment and while little data on lifetime testing has appeared to date, estimates in the 10,000-hour range have been heard.

Near IR Wavelength Devices

The near IR wavelength passband of 0.7-1.1 μm is not as familiar to traditional thermal imager users as the other two wavebands since its use is restricted to objects at temperatures above about 600°C.

In 1995, at Thermosense XVII, researchers at BHP Steel in Australia reported³ the development of a practical near IR thermal imager using Silicon CCD (Charge-Coupled Device) FPA detector array devices (640 x 480). They gave several interesting examples of their use in steel mill areas such as hot rolling and continuous casting. One very interesting application reported was the detection of iron in a slag stream runner from a blast furnace. The latter application was based on the ability to detect the brightness differences because the blast furnace slag had an emissivity approximately 50% higher than the liquid iron, a use very similar to the one being discussed here. CCD devices are common in many common items such as video camcorders, closed circuit video systems and digital cameras. They are designed for visual use, rather than precise

measurement and have some limitations in terms of pixel to pixel uniformity and “crosstalk” between pixels, especially when near saturation. They are, however, plentiful and inexpensive devices. Detector arrays with 640 x 480 resolution capability, or better, are the norm.

General Electric Company (USA) received a patent⁴ in 1987 for a silicon CID (Charge-Injection Device) array thermal imaging camera that overcame some of the limitations of CCD arrays used in thermal imaging and offers a unique device, one that can achieve uniform, long-lived calibration. Like most silicon photo detectors, it has an MTBF in the range of 10,000-100,000 hours and resolution of 640 x 480, as well. It became available commercially from Mikron Instrument Company, Inc⁵ in the 1990’s as a fully developed, industrially packaged line of continuous duty measuring thermal imagers with a standard complement of mounting, purging and cooling accessories. Mikron is well known for its range of industrial infrared radiation thermometers and its expertise in blackbody calibration furnaces and standards devices.

The near IR wavelengths are most familiar to those who are involved in noncontact temperature measurements in high temperature applications, e.g., greater than 600°C, such as those found in steel mills. Spot temperature measurement devices using silicon photovoltaic cells as the fundamental transducer element in 0.7-1.1 μm waveband are quite commonly used in many high temperature processes in steel plants and elsewhere. They have a demonstrated reliability and stability well suited to long term, continuous operation.

Silicon FPA sensors are based on photo junctions in silicon materials so that the actual choice of wavelength passband covers both the visible and the near IR, from 0.4 to 1.1 μm . Thus, the choice of passband for a CID or CCD sensor array is mainly a matter of filter selection.

Perhaps one of the most attractive features of a near IR imager is that fact that commercially available, reasonably priced optics are plentiful.

Other Near IR devices are on the market, such as the 0.9–1.7 μm InGaAs (Indium-Gallium-Arsenide) 320 x 256 pixel cameras available from Sensors Unlimited Inc. (Princeton, NJ), but they have not been yet packaged for heavy-duty industrial use.

Equipment Features Summary

One way to assess the utility of the various waveband choices is to compare key equipment functional and hardware parameters that feature in any system decision. Typical system prices to install and use any of these systems described here lies upwards of \$200,000, a significant sum that must be cost-justified. In addition, such potential expenditures also must compete with other potential corporate capital expenditures so as to maximize the effectiveness of capital spending. Life cycles cost estimates are the usual ones used so as to fully incorporate the long-term advantages offered by more reliable equipment. Lowest first cost is not always the best price, in the long run.

A typical installed system will be required to operate continuously, to have at least two cameras, since BOF facilities typically have two vessels that operate alternately. A display is required at each Operator’s Pouring Station.

Table 1, below, summarizes some of the key hardware features of the three principle types of imaging systems described above.

Table 1. Hardware Summaries of Different Waveband Imaging Systems

Item\Passband	0.7-1.1 μm	3 – 5 μm	8 – 12 μm
Detector Type	Silicon CID	PtSi	Microbolometers
Image Array Size	640 x 480	256 x 256	320 x 240
Optics Material	Glass	Silicon, Germanium	Silicon, Germanium
Cooling Required	Air	Air & Other	Air & Other
MTBF	10,000+	2500(?)	2500(?)
Relative Cost	Low	Very High	Very High
Temp. Accuracy	1% or better	~2-3%	~2-3%

It seems clear to this point that a near IR system will offer the unusual combination of superior hardware features, notably higher image resolution and better MTBF, and lowest system cost, both first and life-cycle. The only questions that remain relate to the technical merits of the different available wavelengths. Is there a difference in the response at different wavelengths? Are the different wavelengths affected by other application parameters, most important being sight path attenuation of the radiances? Is there an optimum choice in wavelength of a system? A look at the theory underlying the measurements, or why and how the application works, will provide the answers.

IV. WHY & HOW IT WORKS

In a nutshell, the method works because there exists a significant difference in the respective apparent temperature of the slag and the steel at all visible and infrared wavelengths. That is a very terse description of this application. A closer look at the details tells a more complete story.

To be precise, the slag and steel differ in spectral radiance temperature. Spectral radiance temperature is the temperature at which an object appears to be if no emissivity correction is made to the received radiance. (It appears to be a blackbody at a lower temperature than it actually is.) The spectral radiance temperature depends upon two key measurement parameters in addition to the actual or true temperature. They are the object's emissivity and the wavelength passband of the device measuring the radiance. The emissivity must be the in-band spectral emissivity, as in nearly all radiation thermometer measurements.

The fundamental equation in radiation thermometry⁶ that applies is the radiance equation:

$$L(\lambda, T_\lambda) = \varepsilon * L(\lambda, T)$$

Where: $L(\lambda, T)$ is the radiance of a object at temperature T and wavelength λ , in watts/(sq. meter- μ m-steradian),
 ε is the object's emissivity at temperature T and wavelength λ , and
 T_λ is the spectral radiance temperature of the object in Kelvin.

Since the radiance, $L(\lambda, T)$, is given by Planck's law, it follows that:

$$\frac{1}{(e^{c_2/\lambda T_\lambda} - 1)} = \frac{\varepsilon}{(e^{c_2/\lambda T} - 1)}$$

Where: c_2 is the second Planck radiation constant, 14387.9 μ m-K.

From which it can readily be shown that:

$$T_\lambda = \frac{c_2 T}{c_2 - \lambda T * \ln(\varepsilon)}$$

Note that while the emissivity enters as a linear factor in the radiance equation, it plays a less significant, logarithmic role in the above temperature equation. Also, the emissivity is not a strong function of temperature but depends upon material and wavelength.

Figure 2 is a plot of spectral radiance temperatures for a 1650°C (1923 K), about 3000°F, object over the range of wavelengths 0.4 to 14 microns for emissivities from 0.9 to 0.1. Notice that the results are expressed in the Absolute Temperature Scale in Kelvin and that at the extremely long wavelengths, a low emissivity object can appear to be quite cold if reflected radiation from the surroundings is neglected (which occurs in special environments such as outer space).

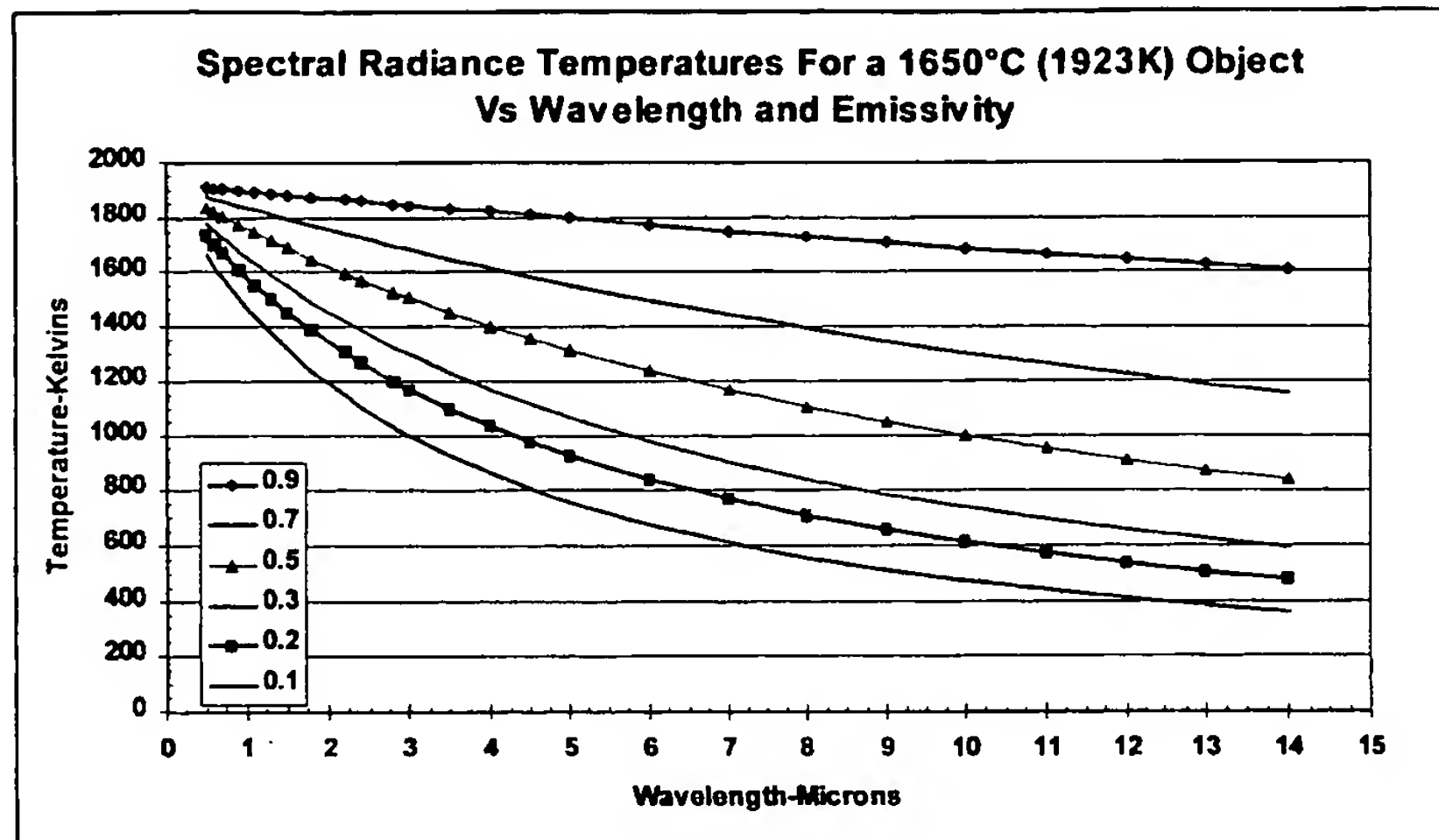


Figure 2

The actual temperature of the steel and slag are relatively high, typically about 1650°C, and they are nearly at the same temperature. (Some workers in the field are convinced that the slag can sometimes be +100°C, or more, hotter than the steel⁷; but this only serves to make the apparent differences greater.)

The steel and slag principally have different radiance or apparent temperatures because their emissivities are different. Slag has a higher emissivity than steel, so it appears hotter even if it is at the same temperature as the steel. Figure 3 is a plot of the estimated spectral emissivities of steel and slag. Note that slag is nearly gray (uniform emissivity versus wavelength) while steel exhibits the decreasing emissivity versus wavelength relation seen in all unoxidized metals⁸. A curve fit to the existing published data shows good agreement to the Hagen-Rubens prediction of an inverse square root relationship between emissivity and wavelength

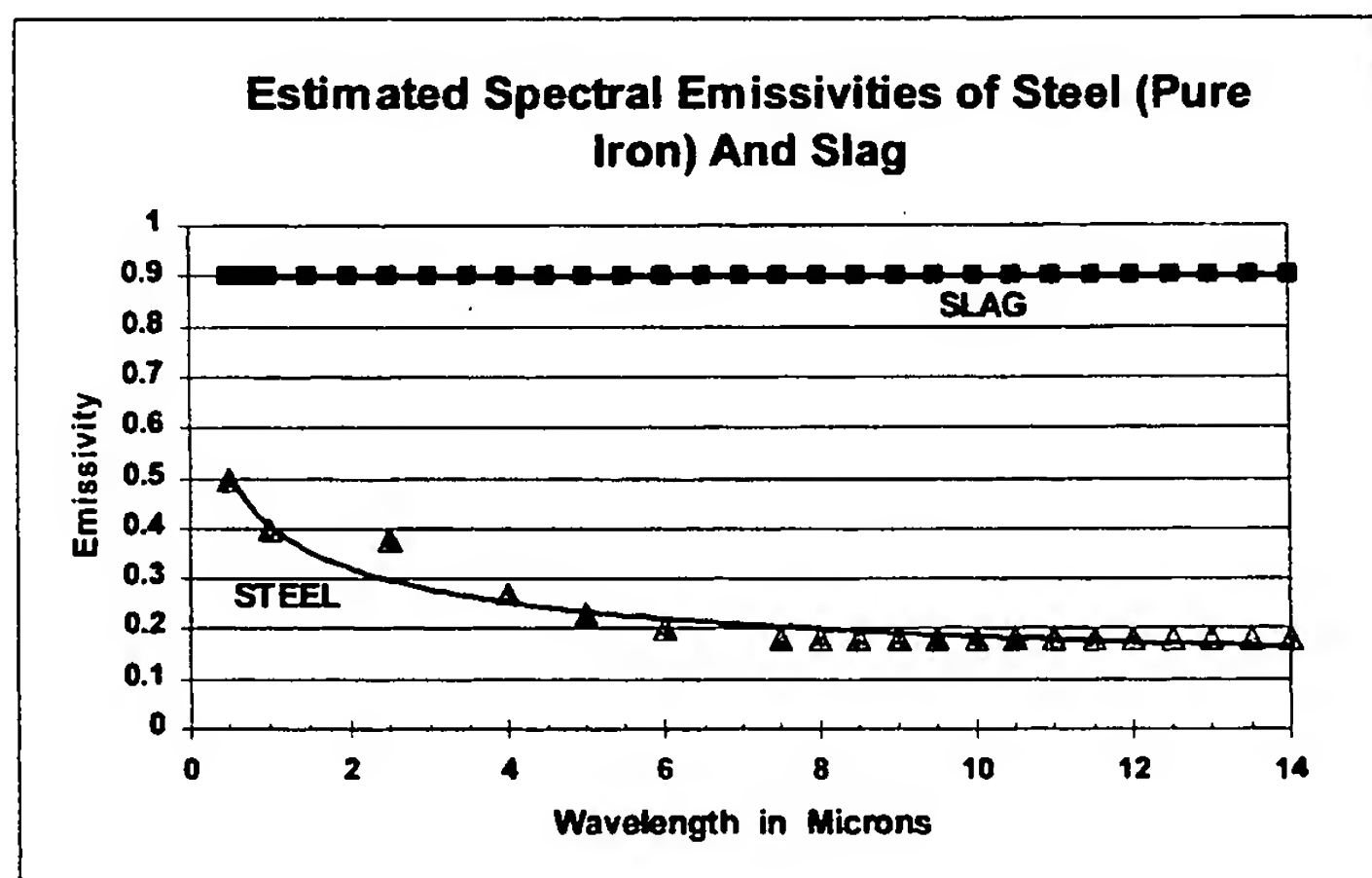


Figure 3

There is a huge amount of thermal energy present at 1650°C and almost any thermal imaging system will be able to record an image even from distances of 30 meters or more or using a high f-number optical system.

Look next at the at the spectral radiance temperatures factoring in the two emissivity curves as shown in Figure 4 which considers the worst-case condition of the two materials at the same temperature.

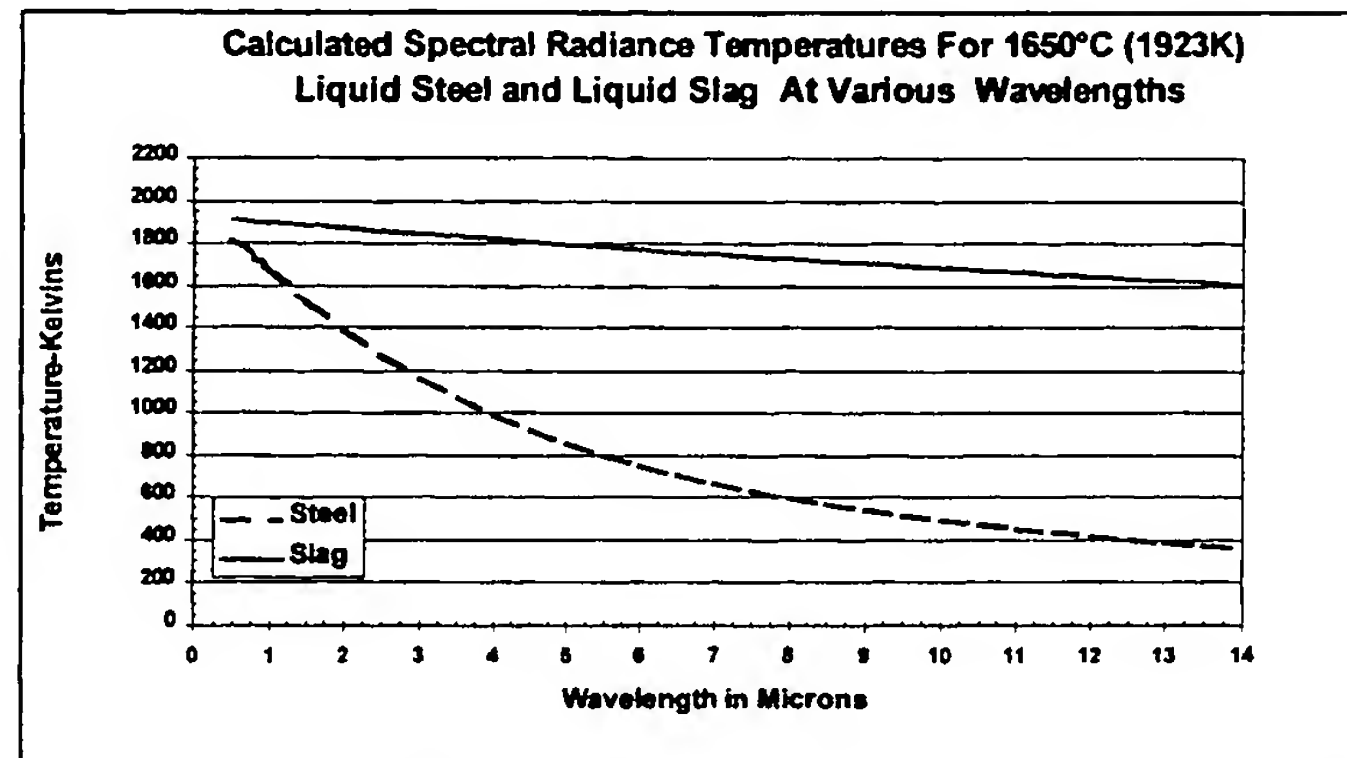


Figure 4

The difference in spectral radiance temperatures between the two materials also can be plotted, as shown in Figure 5. The greatest difference in radiance temperature occurs at wavelengths longer than 8 microns, lending more interest in the use of imagers having the long wavelength passbands. Note that there are significant differences at all wavelengths.

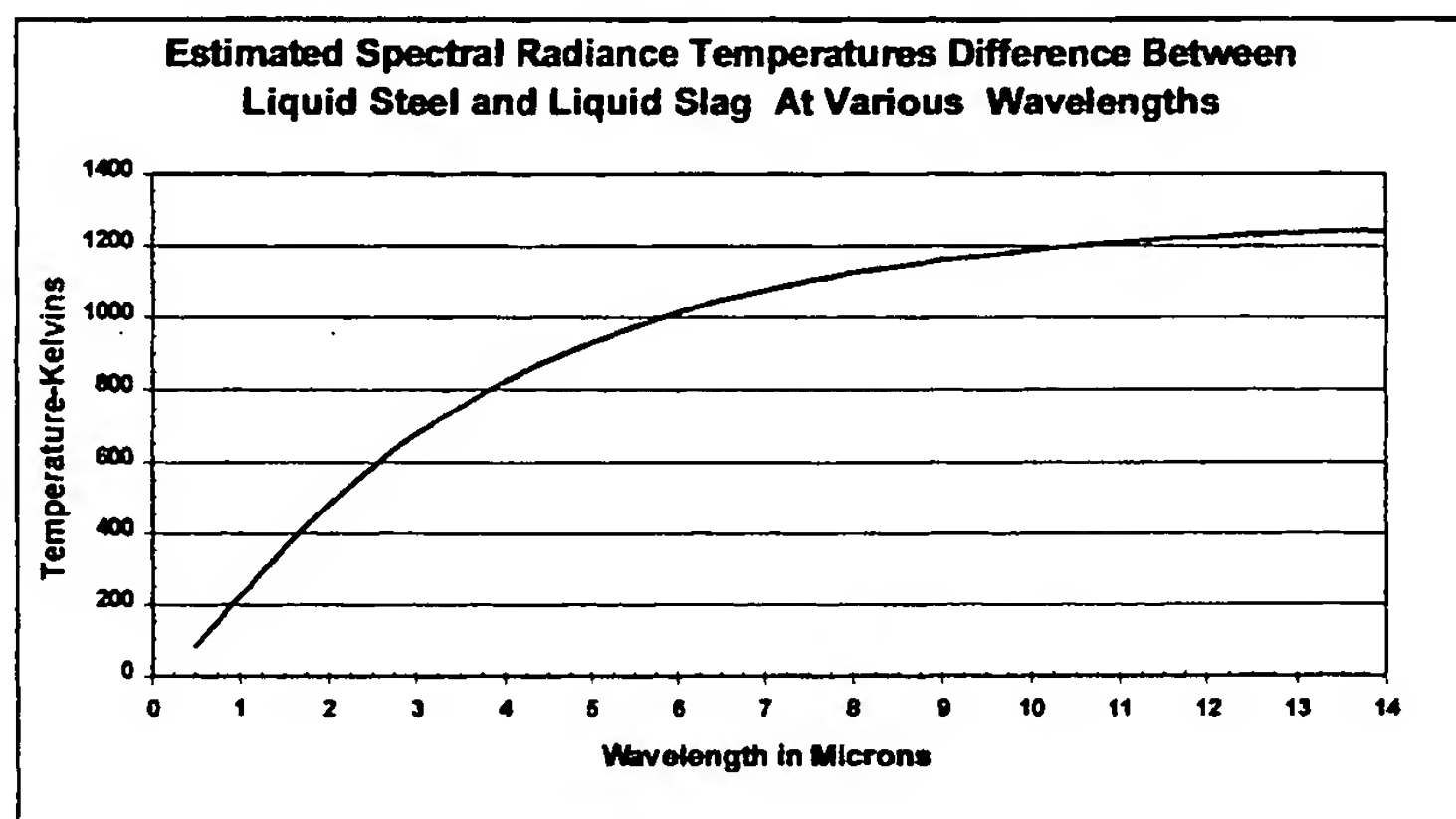


Figure 5

Imager Sensitivity To Sight Path Attenuation

Estimating the effect of sight path attenuation on the temperatures reported by thermal imagers can be done from calculated radiance values since both the emissivity and the net sight path attenuation affect the received radiance linearly. The sum of the in-band radiances received by an uncorrected imager is just the sum of the radiances in the first equation (above) over the wavelength passband of an imager. Tables of spectral radiance for blackbodies are published in many texts on heat transfer and other references^{6,9}. Using the wavebands described below, the in-band radiances are tabulated and shown in Figure 6 for these objects each at 1650°C having the mean in-band spectral emissivity described above.

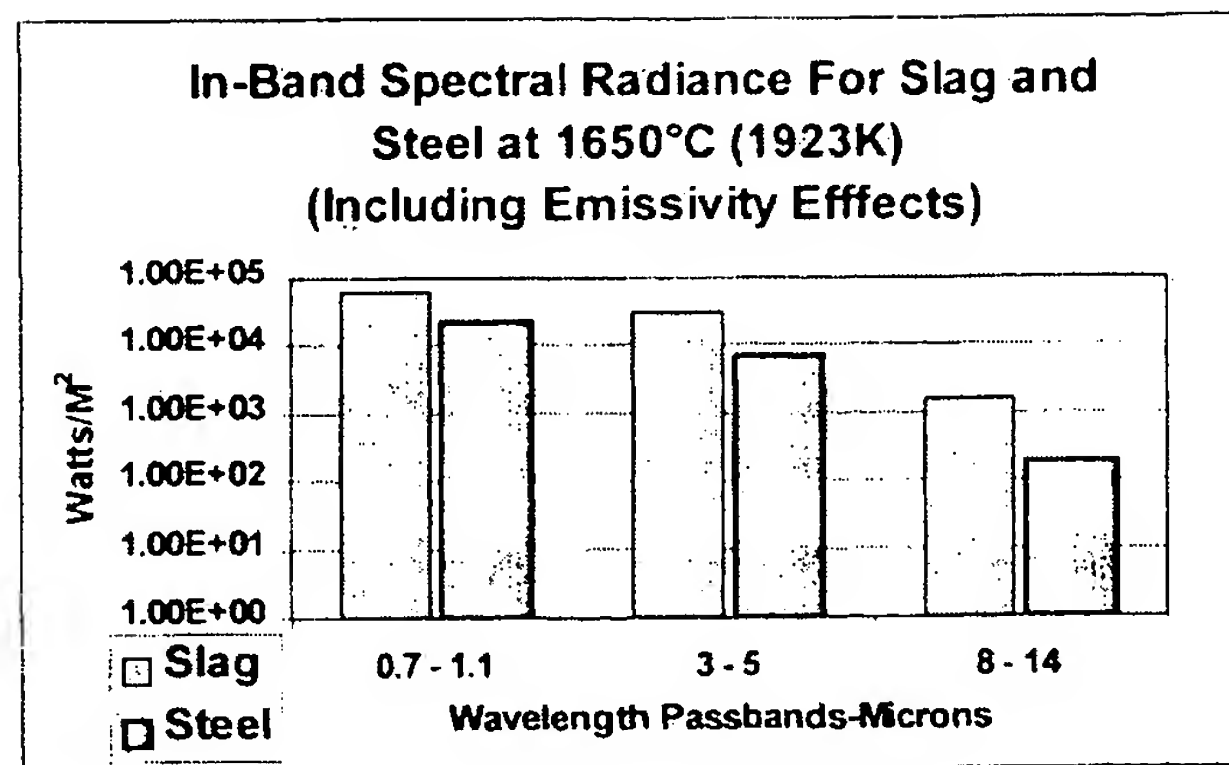


Figure 6

Note in this graph that the radiance scale is logarithmic, in order to show the radiance at the extremes in wavelengths. This is a consequence of Planck's Law, which describes the fact that the radiance increases much faster with temperature at short wavelengths, where short can be defined as those wavelengths on the short wavelength side of the peak in Planck's curve. Since the peak occurs at $\lambda T = 2898 \mu\text{m}\cdot\text{K}$, at 1923 K (1650°C), the peak is at $1.5 \mu\text{m}$. Note, too, that the amount of radiance is a maximum in the shortest wavelength passband and that it is more than an order of magnitude larger than the radiance even in the much wider long wavelength bands. If the interest is principally in contrast, or differences between emitted radiances, then subtracting the values in Figure 6 yields Figure 7, below.

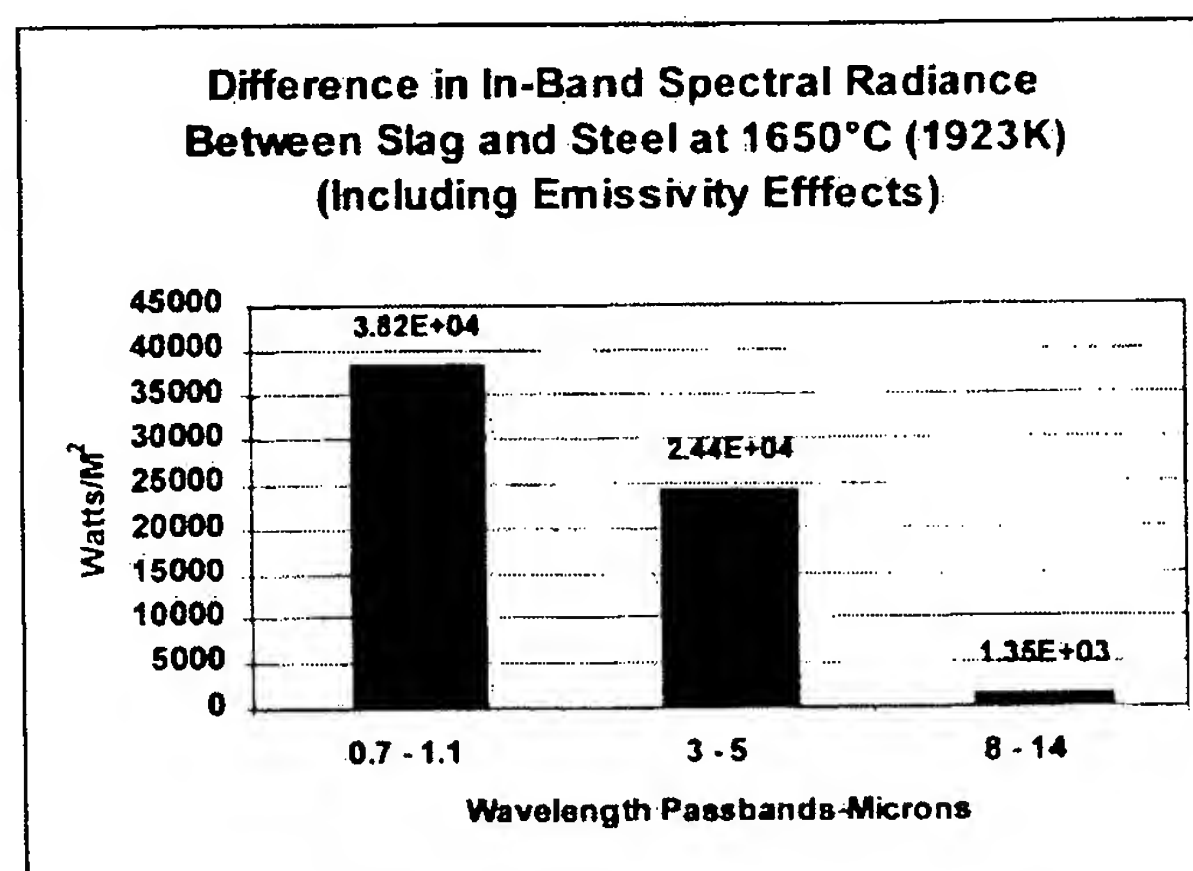


Figure 7

Now the results of the physics of the emission properties of the materials become more obvious. The larger difference in radiance at short wavelengths stems from Figure 6; it is due to the larger radiances at short wavelengths than at longer wavelengths. This is a consequence of nature as described by Planck's Law and the root of the widely used rule-of-thumb in radiation thermometry (for hot objects in cool surroundings): "measure at the shortest wavelength possible to minimize applications effects".

Combining the two sets of data, one for temperature and the other for radiance, will enable development of a quantitative estimate of applications sight path attenuation sensitivity versus imager passband. However, Figure 2 already provides the same information since the effect of sight path attenuation and emissivities are the same (linear reduction in radiance). Sight path attenuation effects can be modeled as an emissivity multiplier. From Figure 2 it is also clear that sight path attenuation will have a very much smaller effect on apparent temperature measurements at short wavelengths than at long.

It is difficult to predict accurately the amount of sight path attenuation likely to be encountered from such interferences as smoke and dust in the actual sight path and dirt accumulation on the optics. Suffice it to say there are conditions during the pouring event, such as during alloy additions, that a great deal of visual attenuation occurs because of clouds of smoke raising from the ladle.

It is, however, obvious that the radiation from the steel and the slag will each experience almost the identical attenuation rate at the same time. Since we are interested in discerning visually between slag and steel at any one moment, *the sight path effect on the difference measurement is a key factor, possibly the most important technical factor in the application*. These are calculated from Figures 2 and 3 and plotted in Figure 8, below.

In Figure 8, it is readily seen that, while long wavelength imagers give large temperature differences between steel and slag, it is also clear that any significant change in sight path properties affects the difference temperatures in the opposite manner. The shortest wavelength system will exhibit a very small variation in the temperature difference, of the order of a few degrees C. The longest wavelength system will show the most variation, almost in direct proportion to the attenuation amount, of the order of hundreds of degrees C, even for a 10% change.

Therefore, there are two distinct differences expected in the operation of thermal imagers operating in different wavebands:

1. Larger apparent differences in temperature between steel and slag occur in the long wavelength systems, and they show large changes in the differences due to even small changes in sight path transmission,
2. Shortest wavelength systems show significant temperature differences between steel and slag that are relatively unaffected by sight path changes.

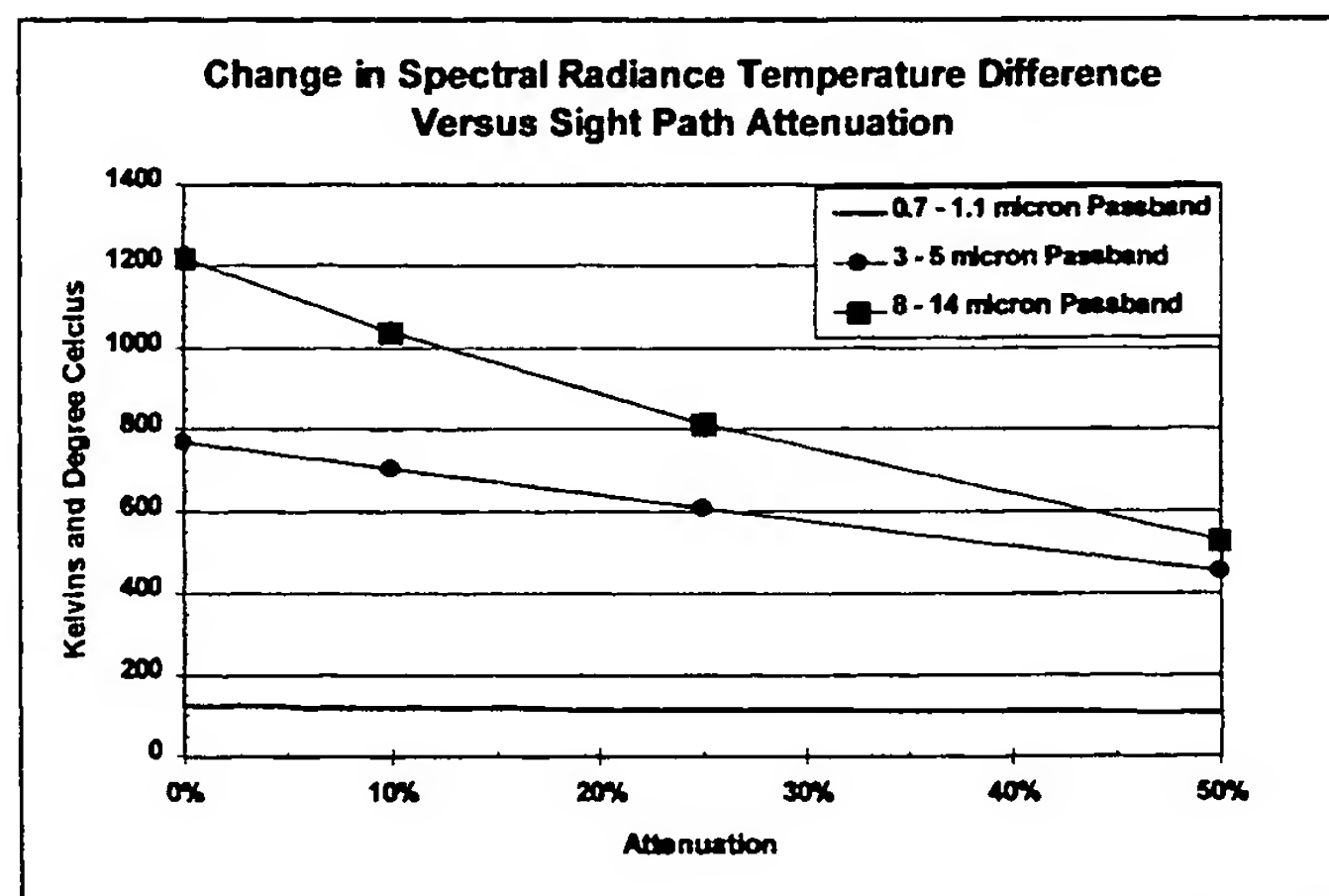


Figure 8

Given the varying and unpredictable amount of sight path attenuation likely to be encountered in this application, the short wavelength passband systems would be the most viable candidate because of its superior repeatable measurement capability. Any automatic control system based on this use of IR thermal imaging equipment would need to be based on the same, more repeatable device.

V. CONCLUSIONS

Nearly any thermal imaging system will help improve a BOF Operator's ability to discern the difference between slag and steel, a more detailed analysis shows clearly that there is an optimum technical solution. It is the same as the optimum hardware solution: the Near IR thermal imager.

It seems now, more likely that most steel companies will be considering near IR thermal imaging systems for many reasons. To summarize them they are:

1. High quality, 640 x 480 resolution imaging capability,
2. Ability to measure almost exactly the same temperature difference between steel and slag even at high levels of sight path attenuation,
3. No detector cooling required,
4. Use standard glass optical lens systems,
5. Demonstrated long MTBF,
6. Industrially-designed equipment readily available,
7. Expected low maintenance costs,
8. Significantly lower first costs, and,
9. Unlikely to infringe steel company patent.

From the equipment features summary, it is also clear that the Near IR hardware system does, in both the first cost and life cycle cost cases, offer the least costly solution.

This is a relatively rare event, the coincidence of best possible technical solution, best available hardware solution and lowest equipment cost.

What remains is for individual companies to perform their own cost justification studies on the benefits of reduced slag in ladles to determine the payback rate for equipment investment. There are no development costs involved in the decision since state-of-the-art equipment exists and is commercially available. The only costs involved are engineering costs to install equipment and interface it with existing plant computers and utilities.

REFERENCES

1. US Letters Patent No.4, 222,506, "Molten Steel Outflow Automatically Controlling Device", Sakashita, T, and I. Yamazaki (1980).
2. U. S. Letters Patent No. 5,968,227, "System and Method For Minimizing Slag Carryover During The Tapping of a BOF Converter in The Production of Steel", Goldstein, D. A. et al (1999).
3. Chen, J. and R. Barrow, "Novel Applications of Thermal Imaging in The Steel Industry" SPIE Vol. 2473, Thermosense XVII, 289-294 (1995).
4. US Letters Patent No.4, 687,344, " Imaging Pyrometer", Lillquist, R.D. (1987).
5. "The Pyro-imager Model 9100", Product Data Sheet, Mikron Instrument Company, Inc, Oakland NJ, (1999).
6. DeWitt, D. P. and F. P. Incropera, "Physics of Thermal Radiation" Chapter 1 in Theory and Practice of Radiation Thermometry, Editors, D.P. DeWitt and E.A. Nutter, Wiley-Interscience, John Wiley & Sons, New York (1989).
7. Private Communication, R.O. Russell, LTV Steel Company. Inc.
8. DeWitt, D. P. and J.C. Richmond, "Thermal Radiative Properties of Materials", Chapter 2 in Theory and Practice of Radiation Thermometry, Editors, D.P. DeWitt and E.A. Nutter, Wiley-Interscience, John Wiley & Sons, New York (1989).
9. Siegel, R. and J.R. Howell, Thermal Radiation Heat Transfer, 2nd Edition, McGraw-Hill Book Company, New York (1981).